Assessment of numerical methods for estimating the wall shear stress in turbulent Herschel–Bulkley slurries in circular pipes

Mehta, Dhruv; Thota Radhakrishnan, Adithya Krishnan; van Lier, Jules B.; Clemens, Francois H.L.R.

Important note
To cite this publication, please use the final published version (if applicable).
Please check the document version above.

Assessment of numerical methods for estimating the wall shear stress in turbulent Herschel–Bulkley slurries in circular pipes

Dhruv Mehta, Adithya Krishnan Thota Radhakrishnan, Jules B. van Lier & Francois H.L.R. Clemens

Published online: 24 Jul 2020.

Submit your article to this journal

Article views: 927

View related articles

View Crossmark data

Research paper

Assessment of numerical methods for estimating the wall shear stress in turbulent Herschel–Bulkley slurries in circular pipes

DHRUV MEHTA, Postdoctoral Researcher, *Sanitary Engineering, Delft University of Technology, Delft, the Netherlands*
Email: *d.mehta@tudelft.nl (author for correspondence)*

ADITHYA KRISHNAN THOTA RADHAKRISHNAN, Doctoral Researcher, *Sanitary Engineering, Delft University of Technology, Delft, the Netherlands*
Email: *a.k.thotaradhakrishnana@tudelft.nl*

JULES B. VAN LIER [ID], Professor, *Sanitary Engineering, Delft University of Technology, Delft, the Netherlands*
Email: *j.b.vanlier@tudelft.nl*

FRANCOIS H.L.R. CLEMENS [ID], Professor (TU Delft), *Deltares, The Netherlands and Sanitary Engineering, Delft University of Technology, Delft, the Netherlands*
Email: *f.h.l.r.clemens@tudelft.nl*

ABSTRACT
This article concerns the turbulent flow of Herschel–Bulkley slurries through circular horizontal pipes; in particular, that of concentrated domestic slurry obtained upon separation of domestic waste water and reduction in the use of water for domestic purposes. Experiments with a rheologically equivalent clay (kaolin) slurry indicated a non-Newtonian behaviour of the Herschel–Bulkley type. A modified wall function was developed to enable the Reynolds-averaged Navier–Stokes simulation of Herschel–Bulkley slurries to estimate the wall shear stress. Despite the accuracy achieved, the use of Reynolds-averaged Navier–Stokes models for an entire waste water system is impractical. Therefore, this article assesses the accuracy of semi-empirical models in estimating frictional losses. It also discusses possible modifications of existing models to encompass Herschel–Bulkley behaviour. An evaluation suggests that most existing models deliver estimates of comparable accuracy; however, the probability of these estimates being reliable, while accounting for experimental errors in quantifying the actual frictional losses, is rather low.

Keywords: Domestic slurry; Herschel–Bulkley; non-Newtonian; pipe flow; Reynolds-averaged Navier–Stokes; urban hydraulics

1 Introduction

Domestic slurry can be concentrated by in-house separating concentrated streams from more diluted streams and by reducing the volume of water used for domestic appliances, particularly for the flushing of toilets, for example, by using vacuum as a means of transport. Doing so not only saves water but also increases the concentration of the nutrients and biomass in the slurry, facilitating their onsite recovery through downstream waste water treatment (Thota-Radhakrishnan et al., 2018; Zeeman & Kujawa-Roeleveld, 2011). An important parameter in the design of a waste water transport system for concentrated domestic slurry, is the pressure drop due to the frictional losses incurred by the slurry. This makes the knowledge of the pressure drop and the relationship it bears with the slurry's rheology, volume flow rate and temperature, a prerequisite for design. The co-authors conducted experiments on clay (kaolin) slurries that were established as being rheologically similar to concentrated domestic slurry. It was noticed that these slurries showed a non-Newtonian behaviour of the Herschel–Bulkley (HB) type (Thota-Radhakrishnan et al., 2018).

1.1 *Non-Newtonian fluids*

For a Newtonian fluid, the shears stress is directly proportional to the strain rate, where the constant of proportionality depends only on the temperature and pressure. The relation reads:

$$\boldsymbol{\tau} = \mu \dot{\boldsymbol{\gamma}} \tag{1}$$

where μ is the molecular viscosity that depends on the temperature and pressure, $\boldsymbol{\tau}$ is the stress tensor and $\dot{\boldsymbol{\gamma}}$ is the strain rate tensor defined as:

$$\dot{\boldsymbol{\gamma}} = \nabla \boldsymbol{u} + \nabla \boldsymbol{u}^T \tag{2}$$

where $\boldsymbol{u}$ is the velocity vector and $\nabla \boldsymbol{u}$ its gradient tensor or $\partial u_j / \partial x_i$ and T denotes a transpose. A non-Newtonian fluid, on the other hand, follows a relationship that reads:

$$\boldsymbol{\tau} = \eta(|\dot{\boldsymbol{\gamma}}|)\dot{\boldsymbol{\gamma}} \tag{3}$$

wherein the function $\eta(|\dot{\boldsymbol{\gamma}}|)$ is not related to $\dot{\boldsymbol{\gamma}}$ but its second invariant $|\dot{\boldsymbol{\gamma}}|$, called the shear rate. One can obtain the shear rate from the strain rate tensor using:

$$|\dot{\boldsymbol{\gamma}}| = \sqrt{\frac{1}{2}\{\dot{\boldsymbol{\gamma}}{:}\dot{\boldsymbol{\gamma}}\}} \tag{4}$$

$$\dot{\boldsymbol{\gamma}}{:}\dot{\boldsymbol{\gamma}} = \mathrm{tr}(\dot{\boldsymbol{\gamma}}^T\dot{\boldsymbol{\gamma}}) \tag{5}$$

In Eq. (3) η is the apparent viscosity that, unlike the molecular viscosity, depends not only on the fluid's temperature and pressure but also the flow conditions such as the shear rate and even the duration of the shear (Chabbra & Richardson, 1999).

Herschel and Bulkley (1926) report the behaviour of certain non-Newtonian fluids that show two irregular properties. Firstly, these fluids require a threshold stress, called the yield stress, to flow at all. Secondly, once the yield stress is exceeded, causing the fluid to flow, the apparent viscosity of the fluid reduces with increasing shear rate; a property now called pseudoplasticity or shear-thinning. Owing to the mentioned properties, the fluids studied by Herschel and Bulkley (1926) are now known as HB or yield pseudoplastic fluids. Equation (3) in the case of an HB fluid reads (for an isotropic fluid):

$$\boldsymbol{\tau} = \boldsymbol{\tau}_y + m\dot{\boldsymbol{\gamma}}^n \tag{6}$$

where $\boldsymbol{\tau}_y$ is the yield stress, m is the fluid consistency index, n is the fluid behaviour index and $\boldsymbol{\tau}$ is the magnitude of the shear stress. For details on these parameters, the readers are referred to Chabbra and Richardson (1999). It is important to note that the stress and shear rate terms in Eq. (6) are scalars and given that an HB fluid only flows once the yield stress is exceeded, the equation is only valid when $|\boldsymbol{\tau}| = \boldsymbol{\tau} \geq \boldsymbol{\tau}_y$; else if $\boldsymbol{\tau} \leq \boldsymbol{\tau}_y$, $|\dot{\boldsymbol{\gamma}}| = \boldsymbol{\gamma} = 0$. Equation (6) can also be expressed in three dimensions in full tensor notation as Oldroyd (1947):

$$\boldsymbol{\tau} = \left(\frac{\boldsymbol{\tau}_y}{|\dot{\boldsymbol{\gamma}}|} + m\dot{\boldsymbol{\gamma}}^{n-1}\right)\dot{\boldsymbol{\gamma}} \tag{7}$$

Experiments conducted by the co-authors suggested that the slurry possesses an HB behaviour. Mehta et al. (2018) proposed how experimentally-determined rheological parameters could be used in combination with CFD to estimate the wall shear stress experienced by an HB slurry in turbulent flow through a
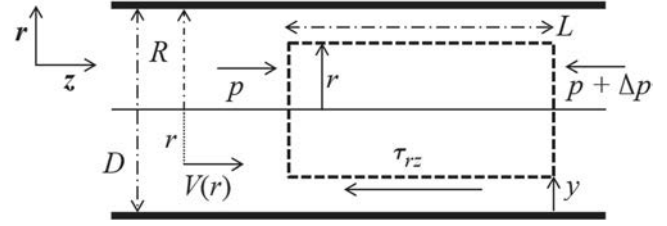

Figure 1　A schematic of the longitudinal section of circular horizontal pipe (Chabbra & Richardson, 1999)

pipe. This article, however, concentrates on alternatives to CFD for estimating the wall shear stress using the same rheological information.

1.2　Pipe flow of HB fluids

Figure 1 is a longitudinal section of a circular pipe with its wall shown as the thick black lines. The pipe has a radius R (and a diameter D). An arbitrary distance from the pipe's centreline is r. The flow is from the left to right along the axis marked as z. Consider a cylinder of radius $r < R$ of length L that is coaxial to the pipe and inside it; its longitudinal section is shown with the dotted line.

The pressure drop across this imaginary cylinder is Δp. This pressure drop is the result of the shear stress acting along the curved surface of the cylinder against the direction of the flow, indicated in Fig. 1 as $\boldsymbol{\tau}_{rz}$.

One can derive:

$$\boldsymbol{\tau}_{rz} = \left(\frac{\Delta p}{L}\right)\frac{r}{2} \tag{8}$$

Further, using Eq. (8) one can obtain the shear stress at the wall or $\boldsymbol{\tau}_w$ by replacing r with R. An important quantity that determines the shear stress is the flow velocity V that is defined as:

$$V = \frac{Q}{\pi R^2} \tag{9}$$

where Q is the volumetric flow rate that can be obtained by integrating the radial distribution of the axial velocity or $V_z(r)$ across incremental annuli of radius r and thickness dr as:

$$Q = \int_2^R 2\pi r V_z(r)\,\mathrm{d}r \tag{10}$$

For a laminar flow of an HB fluid, Eqs (6), (8) and (10) provide an implicit relation between $V(r)$ and $\boldsymbol{\tau}_w$ (Skelland, 1967) :[1]

$$v(r) = \frac{nR}{n+1}\left(\frac{\boldsymbol{\tau}_w}{m}\right)^{1/n}\left\{(1-\zeta)^{(n+1)/n} + \left(\frac{r}{R}-\zeta\right)^{(n+1)/n}\right\} \tag{11}$$

where $\zeta = \boldsymbol{\tau}_y/\boldsymbol{\tau}_w$. Using Eq. (11), one can calculate the wall shear stress for a set of rheological parameters, flow velocity and pipe diameter. However, this cannot be done for turbulent

flows. For details on the laminar solutions and basics principles of non-Newtonian fluids, the readers are referred to Bird et al. (1987, 1983).

2   Semi-empirical models

Various semi-empirical methods have been proposed that enable the quantification of wall shear stress for non-Newtonian fluids of various types, in turbulent flows. Heywood and Cheng (1984) and Assefa and Kaushal (2015) provide a review of various semi-empirical pipe flow models for both laminar and turbulent regimes of various non-Newtonian fluids. This article considers the models proposed by Tomita (1959), Dodge and Metzner (1959) (DM), Torrance (1963), Thomas and Wilson (1987); Wilson and Thomas (1985) (WT) and Slatter (1995). Of these models only WT, Torrance and Slatter included the yield stress in their formulations. Tomita and DM derived their models for power-law fluids, which do not possess a yield stress but have a behaviour index that is not unity.[2] For brevity, references will not be repeatedly quoted. More details on the topics discussed here are well-summarized in Skelland (1967).

2.1   *Tomita*

Tomita (1959) derived two models, one for power-law (PL) fluids and the second for Bingham plastic (BP) fluids, which have a behaviour index $n = 1$ but possess a non-zero yield stress.[3] In either case, Tomita assumed that certain properties of laminar flows of these fluids (velocity profile), also hold for turbulent flows. Based on this assumption, Tomita derived a relationship between the frictional loss and the flow properties. This section describes the derivation and its extension to HB fluids.

Before proceeding with the description of Tomita's models, it is imperative to have a good understanding of what happens when a circular pipe carries a fluid with a non-zero yield stress (either HB or BP). Figure 2 depicts a possible velocity profile of fluid with a non-zero yield stress. As per Eq. (8), at the centreline where $r = 0$, the shear stress is also 0. Further, Eq. (8) dictates that the shear stress is directly proportional to the radial distance from the centreline. Therefore, the shear stress reduces from its maximum value at the wall to zero at the centreline. In doing so, there would exist a region near the centreline, within which the shear stress would be less than the yield stress of the fluid. As a result, an unyielding region is formed near the centreline and the fluid within this region is transported as a plug, thereby reducing the amount of energy lost in turbulence friction when compared to a "Newtonian" velocity profile.

The radial distance at which the plug is formed, r_p, can be obtained by setting τ_{rz} as τ_y at $r = r_p$ and τ_{rz} as τ_w at $r = R$, which results in:

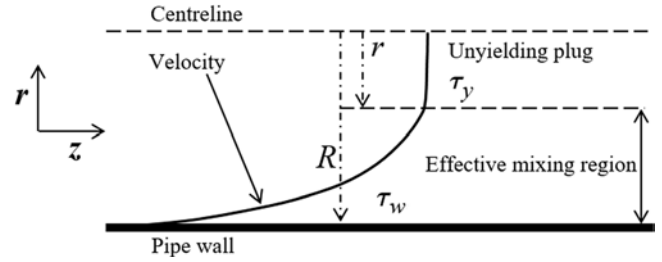$$\zeta = \frac{\tau_y}{\tau_w} = \frac{r_p}{R} \tag{12}$$

Figure 2   The velocity profile of a fluid with a non-zero yield stress inside a circular pipe

Tomita's approach begins with the laminar equations to find a relationship between the average flow velocity V and the rheological properties of the fluid in question (PL and BP, in this case). For a BP fluid:

$$V = \frac{R\tau_y}{m} = \underbrace{\frac{\zeta^4 - 4\zeta + 3}{12\zeta}}_{\alpha} \tag{13}$$

Further, the velocity of the plug or v_p in the region $0 \leq r \leq r_p$ is:

$$v_p = \frac{R\tau_y}{m} \frac{(1 - \zeta)^2}{2\zeta} \tag{14}$$

whereas the velocity at a radial distance r in the region $r_p \leq r \leq R$ is:

$$v(r) = \frac{\tau_y}{2r_p m}(R^2 - 2Rr_p + 2rr_p - r^2) \tag{15}$$

Next, the total shear stress at a distance r, which must equal the pressure gradient, is expressed as the sum of the laminar and turbulent contributions, in keeping with Prandtl's theory (Prandtl, 1933). For a BP fluid:

$$\tau_y + m\dot{\gamma} + \overline{\rho u'v'} = \left(\frac{\Delta p}{L}\right)\frac{r}{2} \tag{16}$$

where ρ is the density of the fluid and $\overline{\rho u'v'}$ is the Reynolds stress. When integrated for a laminar flow (hence, neglecting the Reynolds stress), Eq. (16) leads to the following relationship for pressure loss (see Assefa and Kaushal (2015) for details):

$$\left(\frac{\Delta p}{L}\right)_B = \frac{2Vm}{R^2 \zeta \alpha} \tag{17}$$

After normalizing Eq. (16), two non-dimensional numbers were obtained, which for the laminar flow of BP fluids are related through:

$$\frac{\rho V^2}{\tau_y} = \frac{\rho VR}{m}\alpha \tag{18}$$

The right-hand side of Eq. (18) holds similarity to the Reynolds number. Tomita used this similarity to analyse the turbulent flow of a BP fluid as an imaginary laminar flow with an average flow

velocity V equal to that of a turbulent flow. This led to the deduction of a suitable friction factor for BP fluids. For brevity, the analysis is described here in brief.

The pressure gradient in case of a Newtonian fluid can be related to V, D and ρ through:

$$\frac{1}{\rho}\frac{\Delta p}{L} = \frac{4f_N}{2D}V^2 \tag{19}$$

where f_N is the Fanning friction factor for a Newtonian fluid. Tomita further proposed that the energy dissipation for a BP, as opposed to a Newtonian fluid, is only due to the viscosity acting outside the plug region; therefore, V^2 (formally $V|V|$) in Eq. (19) should represent the average velocity outside the plug. As a result, Eq. (19) is modified as:

$$\frac{1}{\rho}\frac{\Delta p}{L} = \frac{4f_*}{2D}V_*^2 \tag{20}$$

V_*^2 is obtained by integrating the square of Eq. (15) in the region $r_p \leq r \leq R$ as:

$$V_*^2 = \frac{2\pi}{\pi R^2}\int_{r_p}^{R} Rrv^2(r)\,\mathrm{d}r = \frac{\tau_w^2 R^2}{60m^2}(1-\zeta)^4(5+6\zeta-11\zeta^2) \tag{21}$$

Further, using $\zeta = \tau_y/\tau_w$ in Eq. (13), one can relate V_*^2 and V^2 through:

$$V_*^2 = \frac{4}{3}\cdot\frac{9}{5}\underbrace{\frac{(5+6\zeta-11\zeta^2)}{(3+2\zeta+\zeta^2)^2}}_{F(\zeta)}V^2 \tag{22}$$

Therefore, the friction factor can now be defined on the basis of similarity as:

$$\frac{1}{\rho}\frac{\Delta p}{L} = \frac{4f_B}{2D}V^2 F(\zeta) \tag{23}$$

where f_B is the friction factor for a BP fluid. Tomita considered simplifying $F(\zeta)$ as $(1-\zeta)$. Further, Fanning's relationship for a Newtonian fluids implies:

$$f_N \mathsf{Re} = 16 \tag{24}$$

which Tomita proposed must also be satisfied by BP fluids described using an appropriate friction factor and Reynolds number. Therefore, using Eqs (17) and (22)–(24), Tomita obtained the following:

$$f_B = \frac{\tau_w}{\frac{1}{2}\rho V^2 F(\zeta)} \tag{25}$$

$$\mathsf{Re_B} = \frac{\rho DV}{m}4\zeta\alpha F(\zeta) = \frac{\rho DV}{m}F(\zeta)\frac{(\zeta^4-4\zeta+3)}{3} \tag{26}$$

As mentioned earlier, $F(\zeta)$ in Eqs (25) and (26) was simplified as $(1-\zeta)$ (Tomita, 1959). Tomita also carried out the above

procedure for a PL fluid to obtain f_P and $\mathsf{Re_P}$ such that:

$$f_P = \frac{\tau_w}{\frac{1}{2}\rho V^2}\underbrace{\frac{4}{3}\frac{(2n+1)}{(3n+1)}}_{\frac{1}{G(n)}} \tag{27}$$

$$\mathsf{Re_P} = 6\frac{\rho D^n V^{2-n}}{m}\left(\frac{3n+1}{n}\right)^{1-n}\left(\frac{n}{2n+1}\right)\frac{1}{2^n} \tag{1}$$

$$= \frac{1}{8^{n-1}}\frac{\rho D^n V^{2-n}}{m}G(n)\left\{4-\frac{3}{G(n)}\right\}^n \tag{28}$$

$$\left(\frac{\Delta p}{L}\right)_P = 2^{n+2}m\left(\frac{3n+1}{n}\right)^n\frac{V^n}{D^{n+1}} \tag{29}$$

$$f_P \mathsf{Re_P} = 16 \tag{30}$$

The final step involves finding a relation between the mean flow velocity and the wall shear stress. This is done using Eq. (16), in which the turbulent stress is rewritten in terms of the mixing length introduced by Prandtl (1933). Equation (16) then reads:

$$\tau_y + m\dot{\gamma} + \rho\kappa^2 y^2\left(\frac{\partial v}{\partial y}\right)^2 = \left(\frac{\Delta p}{L}\right)\frac{(R-y)}{2} \tag{31}$$

$m\dot{\gamma}$ is neglected (for turbulent flows and to permit the use of the term $(1-\zeta)$ for simplicity) and the right-hand side is rewritten in terms of the wall shear stress leading to:

$$\tau_y + \rho\kappa^2 y^2\left(\frac{\partial v}{\partial y}\right)^2 = \tau_w\left(1-\frac{y}{R}\right) \tag{32}$$

Equation (12) can be used to modify τ_y and rewrite it in terms of τ_w. Another modification needed here for the term $(1-y/R)$. Near the wall, this term is close to unity, so Eq. (32) could be written as:

$$\rho\kappa^2 y^2\left(\frac{\partial v}{\partial y}\right)^2 = \tau_w(1-\zeta) \tag{33}$$

Although the reasoning followed here should ideally hold only when $y \ll R$, Eq. (33) correlates well with experimental data in turbulent regions away from the wall, at least for Newtonian fluids. Tomita made the same assumption for BP fluids and, upon integrating Eq. (33), obtained:

$$\frac{v_p - v}{v_*} = \frac{\sqrt{1-\zeta}}{\kappa}\ln\left\{\frac{R(1-\zeta)}{y}\right\} \tag{34}$$

For succinctness, the steps that follow are not detailed but can be found in Tomita (1959). On integrating Eq. (34), one finds a relation between v_p and V. Further, Eq. (34) is modified as

follows:

$$\frac{v}{v_*} = A\sqrt{1-\zeta} + B\sqrt{1-\zeta}\ln\left\{\mathsf{Re_B}\frac{y}{R(1-\zeta)}\frac{\sqrt{2}u^*}{V\sqrt{F(\zeta)}}\right\}$$
(35)

which, when rewritten using the relationship between v_p and V, reads:

$$\frac{1}{\sqrt{f_B}} = \left(A - \frac{(1-\zeta)(\zeta+3)}{2\kappa}\right)\sqrt{\frac{F(\zeta)(1-\zeta)}{2}} + B\sqrt{\frac{F(\zeta)(1-\zeta)}{2}}\ln(\mathsf{Re_B}\sqrt{f_B})$$
(36)

Finally, with the assumption that for a turbulent flow with high flow velocities V, the wall shear stress would be high enough for $\zeta \ll 1$, implying that the term $\sqrt{F(\zeta)(1-\zeta)}$ becomes close to 1, Eq. (36) was regressed against experimental data points in Tomita (1959) to obtain :

$$\frac{1}{\sqrt{f_B}} = 4\log(\mathsf{Re_B}\sqrt{f_B}) - 0.38$$
(37)

which when $\tau_y = 0$, coincides with the relationship for a Newtonian fluid that was proposed by Nikuradse (1933). Similarly, starting with Prandtl's equation for a PL fluid:

$$m\dot{\gamma}^n + \rho\kappa^2 y^2\left(\frac{\partial v}{\partial y}\right)^2 = \tau_w\left(1 - \frac{y}{R}\right)$$
(38)

while making the assumptions made for BP fluids earlier, Tomita obtained:

$$\frac{v}{v_*} = \frac{1}{\kappa}\ln\left(\frac{R}{y}\right)$$
(39)

Integrating Eq. (39) for a relationship between v_p and V, and following the steps for Eqs (35) and (36), Tomita proposed the PL equivalent for Eq. (36) as:

$$\frac{1}{\sqrt{f_P}} = \left(A - \frac{3}{2\kappa}\right)\sqrt{\frac{G(n)}{2}} + B\sqrt{\frac{G(n)}{2}}\ln(\mathsf{Re_P}\sqrt{f_P})$$
(40)

which, upon regression against experimental data, was presented by Tomita as:

$$\frac{1}{\sqrt{f_P}} = 4\log(\mathsf{Re_P}\sqrt{f_P}) - 0.38$$
(41)

In either case (BP or PL), the friction factor, Reynolds number and the parameter ζ (for BP only) is obtained through the laminar relations detailed at the beginning of this section.

Tomita assumed that these laminar relations also hold for turbulent flows. The authors followed Tomita's procedure to derive an equivalent expression for HB fluids. The process is not detailed here for brevity but is similar to what is mentioned in Tomita (1959). The foremost assumption is that the equivalent friction factor and Reynolds numbers (also ζ in this case), derived for the laminar flow of HB fluids are also assumed to be valid for turbulent flows. These expressions are as follows (see Chabbra and Richardson (1999) for details):

$$v(r) = \frac{nR}{n+1}\left(\frac{\tau_w}{m}\right)^{1/n}\left\{(1-\zeta)^{1+1/n} + \left(\frac{r}{R} - \zeta\right)^{(n+1)/n}\right\}$$
(42)

$$V = \frac{nR}{n+1}\left(\frac{\tau_w}{m}\right)^{1/n}(1-\zeta)^{1+1/n} \times \underbrace{\left\{\frac{n+1}{3n+1}(1-\zeta)^2 + \frac{n+1}{2n+1}2\zeta(1-\zeta) + \frac{1}{n+1}\zeta^2\right\}}_{\alpha_H}$$
(43)

$$v_p = \frac{nR}{n+1}\left(\frac{\tau_w}{m}\right)^{1/n}(1-\zeta)^{1+1/n}$$
(44)

$$\tau_y + m\dot{\gamma}^n + \rho\kappa^2 y^2\left(\frac{\partial v}{\partial y}\right)^2 = \left(\frac{\Delta p}{L}\right)\frac{r}{2}$$
(45)

On removing the turbulent term from Eq. (38), replacing γ as $\partial v/\partial r$ and integrating the equation, one obtains an expression for the pressure gradient, similar to Eq. (17) derived by Tomita:

$$\left(\frac{\Delta p}{L}\right)_H = \frac{2Vm^n}{\alpha_H^n R^{n+1}}\frac{1}{(1-\zeta)^{n+1}}\left(\frac{n+1}{n}\right)^n$$
(46)

For consistency, Eq. (46) reduces to Eq. (17) for $n = 1$. As per Tomita's arguments, the pressure drop should be related to a friction factor, such that the value of the velocity used in Eq. (20) should in a way be obtained as an average of the flow outside the plug, which is directly responsible for frictional losses. Therefore, for an HB fluid, one integrates the square Eq. (42) in the region $r_p \leq r \leq R$ as done in Eq. (21), to obtain a suitable V_*^2, which can be related to Eq. (43) as:

$$V_*^2 = \frac{4}{3}\cdot\frac{3}{4}\cdot\underbrace{\frac{(2n+1)(3n+1)}{(3n+2)}\cdot\frac{(n+1)^2\{3n+2+6n\zeta - (9n+2)\zeta^2\}}{\{(2n+1)(n+1) + 2n(n+1)\zeta + 2n^2\zeta^2\}^2}}_{H(\zeta,n)}V^2$$
(47)

In Eq. (47), the term $H(\zeta, n)$ is a function of both the ratio of the yield stress to the wall stress and the fluid behaviour index for an HB fluid. By setting $n = 1$, one obtains Eq. (22) for a BP fluid and for $\zeta = 0$, one obtains the following for a PL fluid, indicating that Eq. (47) is a consistent extension of Tomita's concept:

$$V_*^2 = \frac{4}{3} \cdot \underbrace{\frac{3}{4}\frac{(3n+1)}{(2n+1)}}_{G(n)} V^2 \tag{48}$$

Extending Tomita's proposal that the equation $f_N \mathrm{Re} = 16$ should also hold for HB fluids with the relevant friction factor and Reynolds number, one obtains the following set of relations for HB fluids:

$$f_H = \frac{\tau_w}{\frac{1}{2}\rho V^2} \frac{1}{H(\zeta, n)} \tag{49}$$

$$\mathrm{Re}_H = 8\frac{\rho V^{2-n}}{m} H(\zeta, n) \left\{ \frac{n}{n+1}\alpha_H R(1-\zeta)^{1+1/n} \right\}^n \tag{50}$$

One can prove $f_H \mathrm{Re}_H = 16$. Next, the steps illustrated through Eqs (32)–(37) are repeated using Eq. (45). For a turbulent flow, the laminar contribution through $m\dot{\gamma}^n$ can be ignored while retaining τ_y, leading to the set of equations Tomita derived for BP fluids. However, the modification done in Eq. (35), can be adjusted for HB fluids leading to :

$$\frac{1}{\sqrt{f_H}} = \left(A - \frac{(1-\zeta)(\zeta+3)}{2\kappa} \right)\sqrt{\frac{H(\zeta, n)(1-\zeta)}{2}}$$
$$+ B\sqrt{\frac{H(\zeta, n)(1-\zeta)}{2}} \ln(\mathrm{Re}_H \sqrt{f_H}) \tag{51}$$

One can verify that Eq. (51) reduces to that for a PL fluid by setting $\zeta = 0$ and to that for a BP fluid by setting $n = 1$. Further, for $\zeta = 0$ and $n = 1$, one must obtain the Nikuradse expression for Newtonian fluids, as Tomita's expression consistently did. This helps one set the values of A and B. The final expression reads:

$$\frac{1}{\sqrt{f_x}} = \left(3.31 - \frac{(1-\zeta)(\zeta+3)}{2\kappa} \right)\sqrt{\frac{H(\zeta, n)(1-\zeta)}{2}}$$
$$+ 2.49\sqrt{\frac{H(\zeta, n)(1-\zeta)}{2}} \ln(\mathrm{Re}_x \sqrt{f_x}) \tag{52}$$

where x can be either of non-Newtonian fluids considered so far (and even a Newtonian fluid with $H(\zeta, n) = 1$ and $\zeta = 1$). Equation (52) must now be solved iteratively to evaluate the wall shear stress for a given non-Newtonian fluid and flow conditions.

2.2　*Dodge and Metzner*

Dodge and Metzner ([1959](#)) (DM) proposed a semi-empirical relationship between the wall shear stress and the average flow

velocity for PL fluids based on extensive dimensional analysis supported by experiments to determine the relevant constants. Their aim was to relate the Fanning friction factor defined by Eq. (19) to the generalized Reynolds number proposed by Metzner and Reed ([1955](#)).

Chilton and Stainsby ([1998](#)) (CS) extended a part of Metzner and Reed's analysis on the generalized Reynolds number (originally meant for laminar flows) and proposed a relevant Reynolds number of turbulent HB fluids. Using experimental data, CS established that the proposed Reynolds number is physically more representative of transitional and turbulent behaviour than Metzner and Reed's generalized Reynolds number.

This article will consider the approaches put forth by DM and CS.

2.2.1　*DM approach extended to HB fluids*

Skelland ([1967](#)) explains the approach followed by DM in a simple manner. First, DM used the Buckingham π theorem (Buckingham, [1914](#)) (dimensional analysis) to establish a relation between v at any radial location (Fig. [1](#)) and the radius of the pipe R, the wall shear stress and the rheological parameters. Next, similar relations were derived between v near the wall and the maximum velocity in the core v_p, and the rheological parameters.

This is followed by a relationship between the velocity defect or $v_p - V$ and the relevant parameters. Ultimately, the equations obtained by using the Buckingham π theorem are combined to relate a suitable friction factor and the flow conditions. For brevity, only the relevant final equations for an HB fluid are described here. The original equations for a PL fluid by DM are described in Skelland ([1967](#)).

A major difference between the analysis of PL fluids by DM and the HB extension here is the presence of a plug. As per Tomita, it is important to consider the region outside the plug as it is in this region that frictional losses actually occur, contributing to the eventual wall shear stress. Therefore, instead of relating the velocities mentioned in the previous paragraphs to the wall shear stress, the velocities will be related to $\tau_w - \tau_y$. The final equations with the symbols used by DM are:

$$\frac{v}{v_{\tau_H}} = \overbrace{h_1}^{0 \le r \le R}\left(\underbrace{v_{\tau_H}^{2-n}\frac{R^n\rho}{m}}_{Z}, \underbrace{\frac{R-r}{R}}_{\xi}, n \right) \tag{53}$$

$$\frac{v}{v_{\tau_H}} = \overbrace{h_2}^{r \to R}(Z\xi^n, n) \tag{54}$$

$$\frac{v_p - v}{v_{\tau_H}} = \overbrace{h_3}^{0 \le r \le r_p}(\xi, n) \tag{55}$$

In the above equations, v_{τ_H} is a special case of the Newtonian definition of friction velocity or v_τ for HB fluids. It will be

defined as:

$$v_{\boldsymbol{\tau}_H} = \underbrace{h_3}_{\sqrt{\boldsymbol{\tau}_w/\rho}} \sqrt{1-\zeta} \tag{56}$$

Further, h_1, h_2 and h_3 are arbitrary functions of the non-dimensional terms contained within the functions brackets and deduced using the Buckingham π theorem. Equations (53)–(55) are combined to obtain the velocity deficit, as done by DM, leading to:

$$\frac{v_p - v}{v_{\boldsymbol{\tau}_H}} = P_n \tag{57}$$

where P_n is a dimensionless function of n. With all these equations, one obtains a relationship between the friction factor of an HB fluid and the flow parameters as (similar to DM) as:

$$\sqrt{\frac{2}{f_{HB}}} = H_1(Z,n) - P_n \tag{58}$$

In Eq. (58), $H_1(Z,n)$ is the value of $h_1(Z,\xi,n)$ at the centreline (or $\xi=1$). f_{HB} is the friction factor for HB fluids, defined in this case as:

$$f_{HB} = \underbrace{\frac{\boldsymbol{\tau}_w}{\frac{1}{2}\rho V^2}}_{f_N}(1-\zeta) \tag{59}$$

Although f_N is the same as previously in Eq. (19), f_{HB} is different from f_H defined using Tomita's procedure through Eq. (49). Further analysis as defined in Skelland (1967) for PL fluids, when done for HB fluids, leads to the following equation, similar to what DM derived but with parameters defined for HB fluids instead of PL fluids:

$$\frac{1}{\sqrt{f_{HB}}} = \underbrace{1.63A_n}_{A_{1n}} \log\left(\underbrace{\frac{\rho D^n V^{2-n}}{m}}_{\mathsf{N}_{\mathsf{Re}}^{\circ}}\right)$$
$$\underbrace{-\,0.49A_n\left(1+\frac{n}{2}\right) + \frac{B_n - P_n}{\sqrt{2}}}_{C_n} \tag{60}$$

where A_n is also a function of n. For a PL fluid, the above equation as proposed by DM contains f_N instead of f_{HB}, as the friction factor for a fluid with zero yield stress is effectively f_N, as per Eq. (59). $\mathsf{N}_{\mathsf{Re}}^{\circ}$ as a modified Reynolds number produces a family of curves depending on the value of n, instead of a unique relationship between the Reynolds number and the friction factor for a laminar flow (Metzner & Reed, 1955). Instead, the protocol put forth by Rabinowitsch (1929) and Mooney (1931) was extended to PL fluids to find a suitable Reynolds number to be used in Eq. (60) (Dodge & Metzner, 1959; Metzner & Reed, 1955).

2.2.2 *A Reynolds number for HB fluids*

The Rabinowitsch–Mooney (RM) criterion establishes that for a laminar flow through a circular tube, the relationship between the pseudo shear rate $8V/D$ and the wall shear stress is unique as long as the shear stress is a function of the shear rate (for time-independent fluids). Just as one uses the Newtonian viscosity determined under laminar conditions for turbulent flows, DM proposed that the unique relationship established for non-Newtonian fluids with the RM criterion could be extended to turbulent flows too. As per RM, the wall shear stress can be related to $8V/D$ as:

$$\boldsymbol{\tau}_w = \frac{D\Delta p}{4L} = m'\left(\frac{8V}{D}\right)^{n'} \tag{61}$$

where n' is obtained using:

$$n' = \frac{\mathrm{d}\ln\left(\frac{D\Delta p}{4L}\right)}{\mathrm{d}\ln\left(\frac{8V}{D}\right)} \tag{62}$$

Metzner and Reed (1955) extended the RM criterion to define the generalized Reynolds number as:

$$\mathsf{N}_{\mathsf{Re\text{-}Gen}} = \frac{\rho D^{n'} V^{2-n'}}{\omega} \tag{63}$$

with $\omega = m'8^{n'-1}$. Further, the RM criterion also states that the strain rate at the wall $\dot{\boldsymbol{\gamma}}_w$ is:

$$\dot{\boldsymbol{\gamma}}_w = \frac{3n'+1}{4n'}\cdot\frac{8V}{D} \tag{64}$$

DM used the above criteria to propose the following Reynolds number for PL fluids to be used in Eq. (60):

$$\mathsf{N}_{\mathsf{Re\text{-}Gen}_{PL}} = \frac{\rho D^n V^{2-n}}{8^{n-1}m\left(\frac{3n+1}{4n}\right)^n} = 8\mathsf{N}_{\mathsf{Re}}^{\circ}\left(\frac{n}{6n+2}\right)^n \tag{65}$$

N_{Re} is defined in Eq. (60). Further, to prevent the loss of generality, the n is replaced with n'. For a PL fluid $n' = n$. Equation (60) when written for PL fluid (as proposed by DM) finally reads:

$$\frac{1}{\sqrt{f_{PL}}} = A_{1n}\log\left(\mathsf{N}_{\mathsf{Re\text{-}Gen}_{PL}}\cdot f_N^{1-n'/2}\right)$$
$$+\,A_{1n}\underbrace{\log\left\{\frac{1}{8}\left(\frac{6n'+2}{n'}\right)^{n'}\right\}}_{C_{n'}} \tag{66}$$

DM determined the constants A_{1n} and $C_{n'}$ as follows:

$$A_{1n} = \frac{4}{(n')^{0.75}}, C_{n'} = \frac{-0.4}{(n')^{1.2}} \tag{67}$$

In terms of consistency, Eq. (66) reduces to the Nikuradse equation for $n' = n = 1$. DM did not extend their results to HB fluids as they demonstrated in Dodge and Metzner (1959) that Eq. (66) also works well for fluids with a non-zero yield stress.

Using the RM criterion, one can derive n' for an HB fluid and obtain a $N_{Re\text{-}Gen_{HB}}$, a procedure that is also followed in Chilton and Stainsby (1998). n' for an HB fluid is:

$$n' = \frac{n\theta}{1 - 3n\theta} \tag{68}$$

where θ is defined as follows (symbols are the ones used in Chilton and Stainsby (1998) for consistency):

$$\theta = \frac{1}{3n + 1}\left\{1 - \underbrace{\frac{1}{2n + 1}}_{a}\zeta - \underbrace{\frac{2n}{(2n + 1)(n + 1)}}_{b}\zeta^2 \right.$$
$$\left. - \underbrace{\frac{2n^2}{(2n + 1)(n + 1)}}_{c}\zeta^3\right\} \tag{69}$$

For brevity, the procedure used to obtain $8V/D$ (for laminar flows as per RM) and m' for a general fluid is not detailed here. For an HB fluid these are:

$$\left(\frac{8V}{D}\right)_{HB} = \frac{4}{m^{1/n}}\frac{1}{\tau_w^3}\theta \tag{70}$$

$$m'_{HB} = \frac{\tau_w^{3n'+1}}{4^{n'}}\frac{1}{\phi^{n'}}m^{n'/n} \tag{71}$$

where ϕ is defined as:

$$\phi = n\tau_w^{3+1/n}(1 - \zeta)^{1/n}\theta \tag{72}$$

Combining the above, one obtains the $N_{Re\text{-}Gen_{HB}}$ as defined by Eq. (63):

$$N_{Re\text{-}Gen_{HB}} = \frac{\rho D^{n'}V^{2-n'}}{8^{n'-1}}\frac{4^{n'}}{\tau_w^{3n'+1}}\frac{\phi}{m^{n'/n}} \tag{73}$$

CS (Chilton & Stainsby, 1998) suggested a simplified version of Eq. (73), which does not contain the parameters m' and n'. Further, Eq. (73) can also be expressed in terms of N_{Re}° as proposed by DM.

$$N_{Re\text{-}Gen_{HB}} = \frac{\rho VD}{m}\frac{1}{\left(\frac{8V}{D}\right)^{n-1}}(4n\theta)^n(1 - \zeta)$$
$$= N_{Re}^{\circ}\frac{(4n\theta)^n(1 - \zeta)}{8^{n-1}} \tag{74}$$

One can verify that Eq. (74) is the same as Eq. (65) should $\zeta = 0$ (PL fluid). It is fair to mention at this point that CS deemed this Reynolds number to not be physically realistic for turbulent flows as the entire derivation was based on a laminar velocity

profile. Instead, they proposed a new Reynolds number based on the wall-effective viscosity defined as the ratio of the wall shear stress to the strain-rate at the wall:

$$\eta_w = \frac{\tau_w}{\dot{\gamma}_w} \tag{75}$$

$\dot{\gamma}_w$ can be calculated from Eq. (6) by setting the shear equal to the wall shear stress, which ultimately provides a way to calculate η_w:

$$\eta_w = \frac{m^{1/n}\tau_w}{(\tau_w - \tau_y)^{1/n}} \tag{76}$$

The procedure for deriving the Reynolds number based on the wall-effective viscosity is illustrated in Chilton and Stainsby (1998); the Reynolds number so obtained is:

$$Re_{CS} = \frac{\rho VD}{\eta_w}4n\theta \tag{77}$$

For extending Eq. (77) to HB fluids, one can use the Reynolds number defined by Eq. (74) or the one defined by CS through Eq. (77).

2.2.3 *Dodge–Metzner equation for HB fluids*

One could extend Eq. (66) to HB fluids by combining Eqs (60), (66) and (74). However, one must bear in mind that DM replaced n with n', which is convenient for PL fluids that entail $n = n'$. DM did not provide a clear explanation as to why every n is replaced with n' and if every replacement is justified. DM however asserted that Eq. (66) should ideally be suitable for non-PL fluids based on a calculation that proves that shear rates that are less than 80% of τ_w account for no more than 7% of the mean velocity that results from frictional losses. Therefore, regions away from the wall have significantly lower (perhaps ignorable) contributions to the mean velocity. An experimental verification of this hypothesis along with more details can be found in Skelland (1967).

Further, as the flow of an HB fluid becomes more turbulent, the value of ζ becomes smaller due to increasing wall shear stress. As a result, θ is nearly $1/(3n + 1)$, reducing n' to n and effectively making Eq. (66) suitable for further analyses. Bearing this and DM's assertion in mind, it is perhaps futile to extend Eq. (66) to HB fluids, and more so for highly turbulent flows. Nonetheless, for less turbulent HB flows where ζ is such that it may not be ignored, an extension of Eq. (66) is warranted.

Assuming that every n can be replaced with n', a consistent extension of Eq. (66) to HB fluids must read:

$$\frac{1}{\sqrt{f_N}} = \frac{4}{(n')^{0.75}}\sqrt{1 - \zeta}\log\left(N_{Re\text{-}Gen_{HB}} \cdot f_N^{1-n'/2}\right)$$
$$- \frac{0.4}{(n')^{1.2}}\sqrt{(1 - \zeta)} \tag{78}$$

Equation (78) shall be referred to as DM-HB. Further, CS suggested a similar equation based on Eq. (77) as:

$$\frac{1}{\sqrt{f_N}} = 4\log\left(\mathsf{N_{Re_{CS}}}\frac{1}{n^2}\frac{1}{(1-\zeta)^4}\sqrt{f_N}\right) - 0.4 \qquad (79)$$

which shall be called CS-HB from hereafter. The following sections briefly describe other approaches in literature for turbulent HB fluids.

2.3   Torrance

As one of the older-known expressions for HB fluids, Torrance (1963) proposed:

$$\frac{1}{\sqrt{f_N}} = \left(0.45 - \frac{2.75}{n}\right) + \frac{1.97}{n}\ln(1-\zeta)$$
$$+ \frac{1.97}{n}\left\{\mathsf{Re_{Bi}}\cdot\left(\frac{3n+1}{4n}\right)^n\cdot f_N^{1-n/2}\right\} \qquad (80)$$

where f_N is the Fanning friction factor defined using Eq. (19) as:

$$f_N = \frac{\boldsymbol{\tau}_w}{\frac{1}{2}\rho V^2} \qquad (81)$$

Finally, the Reynolds number in Eq. (80) $\mathsf{Re_{Bi}}$ is the generalized Reynolds number for a PL fluid used by Bird et al. (1987, 1983), which can be derived from $\mathsf{N_{Re\text{-}Gen}}$ proposed earlier in Metzner and Reed (1955):

$$\mathsf{Re_{Bi}} = \frac{1}{8^{n-1}}\frac{D^n V^{2-n}\rho}{m}\left(\frac{4n}{3n+1}\right)^n \qquad (82)$$

It is immediately noticeable that although Torrance's equation includes the contribution of the yield stress that separates an HB fluid from a PL fluid, the Reynolds number used in the equation does not encompass the yield stress. However, it is likely that Eq. (80) could still provide accurate results at high Reynolds numbers, at which the effect of the yield stress would perhaps be negligible.

2.4   Wilson and Thomas

Wilson and Thomas (1985) and Thomas and Wilson (1987) derived Eq. (83) by relating the thickness of the viscous sublayer (representing the dissipation of energy due to friction) with the ratio of the area under the rheogram of an HB fluid to that of a Newtonian fluid, for the same strain-rate and the wall shear stress:

$$\frac{V}{v_{\boldsymbol{\tau}}} = 2.5\ln\left(\frac{\rho D v_{\boldsymbol{\tau}}}{\eta_w}\right) + 2.5\left\{\frac{(1-\zeta)(1+n)}{(1+n\zeta)2}\right\}$$
$$+ \frac{1+n\zeta}{1+n} + (1.25\zeta^2 + 2.5\zeta - 11.6) \qquad (83)$$

where $v_{\boldsymbol{\tau}}$ is the friction velocity defined as:

$$v_{\boldsymbol{\tau}} = \sqrt{\frac{\boldsymbol{\tau}_w}{\rho}} \qquad (84)$$

2.5   Slatter

Slatter (1995) carried out a comprehensive series of experiments with a wide range of HB fluids. First, the Reynolds number to determine the transition for HB fluids was modified to:

$$\mathsf{Re_{Sl}} = \frac{8\rho V_a^2}{\boldsymbol{\tau}_y + m\left(\frac{8V_a}{D_a}\right)^n} \qquad (85)$$

The denominator of the right-hand side of Eq. (85) is similar to the constitutive relation for an HB fluid, i.e. Eq. (6), but with the strain-rate defined in terms of V_a and D_a, which are:

$$V_a = \frac{Q - Q_p}{\pi(R^2 - r_p^2)} \qquad (86)$$

$$D_a = 2(R - r_p) \qquad (87)$$

Q_p is the volume flow rate through the plug, which can be obtained using Eq. (44) in the case of an HB fluid. The above formulae were further modified to account for the particle roughness within the HB fluids under consideration by Slatter. This roughness was related to the representative size of the particles d_{85}. d_{85} is the diameter at which 85% of the slurry's sample mass is comprised on particles smaller in size than d_{85}. For details on the procedure used to determine the representative size, the readers are referred to Slatter (1995) (and Neill, 1988). A different Reynolds number was defined to account for the particle roughness effect as:

$$\mathsf{Re_R} = \frac{8\rho v_{\boldsymbol{\tau}}^2}{\boldsymbol{\tau}_y + m\left(\frac{8v_{\boldsymbol{\tau}}}{d_{85}}\right)^n} \qquad (88)$$

such that $\mathsf{Re_R} < 3.32$ pertains to a smooth pipe flow (fully-developed turbulent) for which the following relationship holds:

$$\frac{V}{v_{\boldsymbol{\tau}}} = 2.5\ln\left(\frac{R}{d_{85}}\right) + 2.5\ln(\mathsf{Re_R}) + 1.75 \qquad (89)$$

On the other hand, for a rough flow, i.e. $\mathsf{Re_R} > 3.32$:

$$\frac{V}{v_{\boldsymbol{\tau}}} = 2.5\ln\left(\frac{R}{d_{85}}\right) + 4.75 \qquad (90)$$

The use of either Eq. (89) or Eq. (90) requires information on the wall shear stress to calculate $v_{\boldsymbol{\tau}}$ and, therefore, must be solved implicitly. Thus, both of them would be used to estimate the wall shear stress for the experimental test cases considered in this article.

3 Computational fluid dynamics

In contrast with the approaches mentioned in Section 2, a CFD-based approach involves solving the modified Navier–Stokes (NS) equations. The term modified in this context refers to a process through which a solution to NS equations could be more easily obtained by only solving for the most relevant turbulent features in a flow. One such modification, known as Reynolds averaging, provides an insight into the flow's features averaged over a number of instances of the flow, using what are better known as the Reynolds-averaged Navier–Stokes (RANS) equations.

Malin (1997, 1998) used the standard $\kappa - \epsilon$ and $\kappa - \omega$ models to simulate non-Newtonian fluids, using the standard model constants for Newtonian fluids. The turbulent viscosity, however, was dampened near the walls with an *ad hoc* function. Both models delivered similar results for HB fluids, which were, in fact, close to the semi-empirical predictions made by Dodge and Metzner, for Reynolds numbers greater than 10^5. Similarly, Bartosik (2006) used the standard $\kappa - \epsilon$ model with a modification for the eddy viscosity near walls to account for non-Newtonian viscosity. The approach was accurate for HB fluids, even with high yield stresses (hence, a stronger deviation from Newtonian behaviour).

The approach in this article involves using the $\kappa - \epsilon$ and Reynolds stress model (RSM) for modelling the turbulence within a 3-D pipe carrying an HB fluid. These models use a wall function to determine the frictional forces near the pipe's walls that would lead to the eventual loss in pressure, without having to resolve the actual velocity field near the pipe's walls, to determine the frictional loss. However, the wall function that is most often used in such simulations is the standard Newtonian wall function proposed by Launder and Spalding (1974).

Mehta et al. (2018) proposed an equivalent wall boundary condition for HB fluids. This condition was validated using the experiments defined in the next section in terms of the pressure drop across a fixed length of a circular pipe. To make it more comprehensive, the pressure drops were not measured for a simple straight section but for a section containing two 90° bends, one of which was upward-facing. For the convenience of the readers, a succinct derivation has been provided in Appendix 1. For details, the readers are referred to Mehta et al. (2018).

Further, it is important to mention that the ability of CFD in this article has been evaluated solely in terms of predicting the wall shear stress. This is because of three reasons: firstly, the experiments conducted by the authors and other researchers do not provide information on the velocity and turbulence profiles in a pipe carrying turbulent HB fluids. Secondly, the wall shear stress is the parameter that is most relevant for estimating frictional losses. Finally, the nature of turbulence in non-Newtonian fluids, as regards to the fluctuations in the shear stress tensor and the local viscosity, are not completely understood. Hence, a modification to the Newtonian RANS approaches that only incorporates the behaviour near the wall (viscosity) can be

suitable for predicting the wall shear stress but may not be appropriate for analysing the flow towards the centre of the pipe unless the flow is highly turbulent, in which case, the viscous behaviour of the fluid is of minor consequence. Mehta et al. (2019) demonstrated that for high Reynolds numbers, the Newtonian RANS models are accurate for estimating frictional losses, but extending them towards predicting velocity and turbulence profiles will still need experimental verification.

Nonetheless, given that CFD incorporates more physics pertaining to turbulence, wall effects and non-Newtonian behaviour than simple semi-empirical models, its potential as a tool for estimating frictional losses must be evaluated and compared against the former.

4 Experiments

Table 1 presents an overview of the various experimental test cases considered in this article. All cases deal with HB fluids in turbulent flow through circular horizontal pipes. As per Eq. (6) the unit of m for a given behaviour index n, is Pas^n. d_{85} is the diameter of the particle that makes up 85% of the mass of the HB fluid under consideration. This implies that 85% of the HB fluids mass comprises particles smaller in diameter than the reported d_{85}.

Details on the experimental measurements and the associated errors are discussed in detail in Mehta et al. (2018). As regards to the cases S8 through S21, the experimental error in measuring the flow rate through the 100 mm pipe is $\pm 10\,\mathrm{l\,min^{-1}}$, which leads to an error of $\pm 0.02\,\mathrm{m\,s^{-1}}$ in estimating the velocity V. On the other hand, the experimentally-determined value of the wall shear stress bears an error of ± 0.24 Pa that corresponds to 2σ or 95% confidence.

It is important to note that turbulent structures within pipes carrying non-Newtonian kaolin slurries are affected not only by the diameter of the pipe but also the yield stresses and concentrations of the slurries. Thus, it is fair to mention that the experiments and the numerical methods compared in this article must be considered along with the diameters of the pipes and rheology of the slurries tested (Bartosik, 2011).

Table 1   The test-cases considered in this article

Case	ρ (kg m^{-3})	τ_y (Pa)	m	n	D (mm)	d_{85} (μm)
KERS2408[a]	1061	1.04	0.014	0.8	79	28
KERS0608[a]	1071	1.88	0.01	0.84	79	28
S8[b]	1052	0.0014	0.004	0.79	100	32
S12[b]	1068	0.0052	0.007	0.7	100	32
S14[b]	1091	0.049	0.013	0.65	100	32
S17[b]	1113	0.16	0.033	0.6	100	32
S21[b]	1146	0.43	0.083	0.52	100	38

[a] Slatter (1995).
[b] Thota-Radhakrishnan et al. (2018).

Table 2   Abbreviations used for the different models

Model	Abbreviation
Tomita PL	TO-PL
Tomita HB	TO-HB
Dodge and Metzner PL	DM-PL
Dodge and Metzner HB	DM-HB
Chilton and Stainsby HB	CS-HB
Torrance	TR
Wilson and Thomas	WT
Slatter smooth	SS
Slatter rough	SR
RANS	CFD
Experimental data	EX

5   Estimates with the semi-empirical models and CFD

This section presents the results obtained with the semi-empirical models described in Section 2. Table 2 lists the abbreviations used for the various models considered here.

The results are presented as plots of the wall shear stress in Pa vs. the pseudo-shear rate $8V/D$ in s^{-1}. While interpreting the results obtained with RANS (CFD), it is important to bear in mind the limitations of the numerical methods involved. These are illustrated in Mehta et al. (2019) as a sensitivity analysis of the wall boundary conditions proposed in Mehta et al. (2018).

For succinctness, only the results from S10, S17, S21 and KERS2408 are discussed here using Figs 3 and 4. One observes the following:

- CFD provides accurate results in all cases, deviating only at high pseudo-shear rates. It is important to note that the approach used for the CFD analysis must comply with the findings of the sensitivity analysis described in Mehta et al. (2019).
- The TO-PL and its proposed extension to HB fluids, TO-HB, only deliver accurate results for S10 (also for S8 but not shown here). These two cases concern HB fluids with very low yield stress, effectively making them PL fluids. However, in the other cases, both TO-PL and TO-HB provide similar results with nearly overlapping plots.
- DM-PL and its proposed extension to HB fluids, DM-HB, show a behaviour similar to TO, with the PL and HB solutions overlapping each other.
- The CS-HB approach deviates from experimental data as the pseudo shear rate increases.
- All the other remaining approaches, namely TR, WT, SS and SR, produce similar results at low shear rates but tend to deviate from each other as the shear increases (increasing flow velocity). One also observes that SS and SR produce the best results for KERS2408.
- WT and TR approaches lead to overlapping estimates.

The accuracy of SS and SR for KERS2408 is simply explained by the fact that these models were obtained by tuning their parameters using experimental data, of which KERS2408 was a part (Slatter, 1995). Regarding the similarity between the PL and HB approaches of the TO and DM models, one could allude to the interesting hypothesis presented in the original article by DM (Dodge & Metzner, 1959). DM explained that their PL model was applicable to non-power law fluids such as HB fluids too. They proved mathematically that the resulting mean velocity in the pipe is dependent mostly on the shear rates occurring a radial distances $r/R > 0.8$ or the shear occurring in the immediate vicinity of the wall.

Therefore, the region away from the pipe's walls and towards the centreline, where the effect of the yield stress for HB fluids is apparent due to the reducing shear stress, in fact contributes to less than 7% of the mean flow that results. This in turn implies that accounting for the yield stress as an extra parameter for HB fluids as part of the DM approach may not add any value to the DM model. By extension, the same applies to the HB extension of Tomita's PL model, in which the incorporation of the yield stress does not alter the estimates of the wall shear stress. The results presented in Figs 3 and 4 can serve as a proof of the idea put forth by DM.

Finally, as regards to the other models, one cannot assess their accuracy easily as the trends in the estimates they provide are not consistent across the test cases discussed here. Thus, to gain more insight into the accuracy of all the models considered in this study, one must resort to a proper error analysis.

6   Probability

To provide a more meaningful insight into the usability of the various numerical models, it is essential to have knowledge of their accuracies. In this study, various models were used to estimate the wall shear stress for certain experimental conditions of flow velocity and the resulting gradient for a range of HB fluids. However, the uncertainty in the experimental determination of the flow parameters itself was not considered. Further, the trends in the accuracy of the estimates with the various models cannot be assessed qualitatively using the results discussed in the previous section.

The "accuracy" is defined as the closeness of an estimate to the real or known value. Meanwhile, the "precision" is defined as the closeness of the estimates to each other; in effect, a measure of how close repeated estimates (using a model or a apparatus) would be to each other.

Given there is an uncertainty in known value (experimentally reported wall shear stress), one must first estimate the possible deviation in the known value itself, i.e. the precision of the experimental method. Next, based on the values obtained from simulations, one must calculate the distribution in the estimated values and the difference of their mean from the "mean
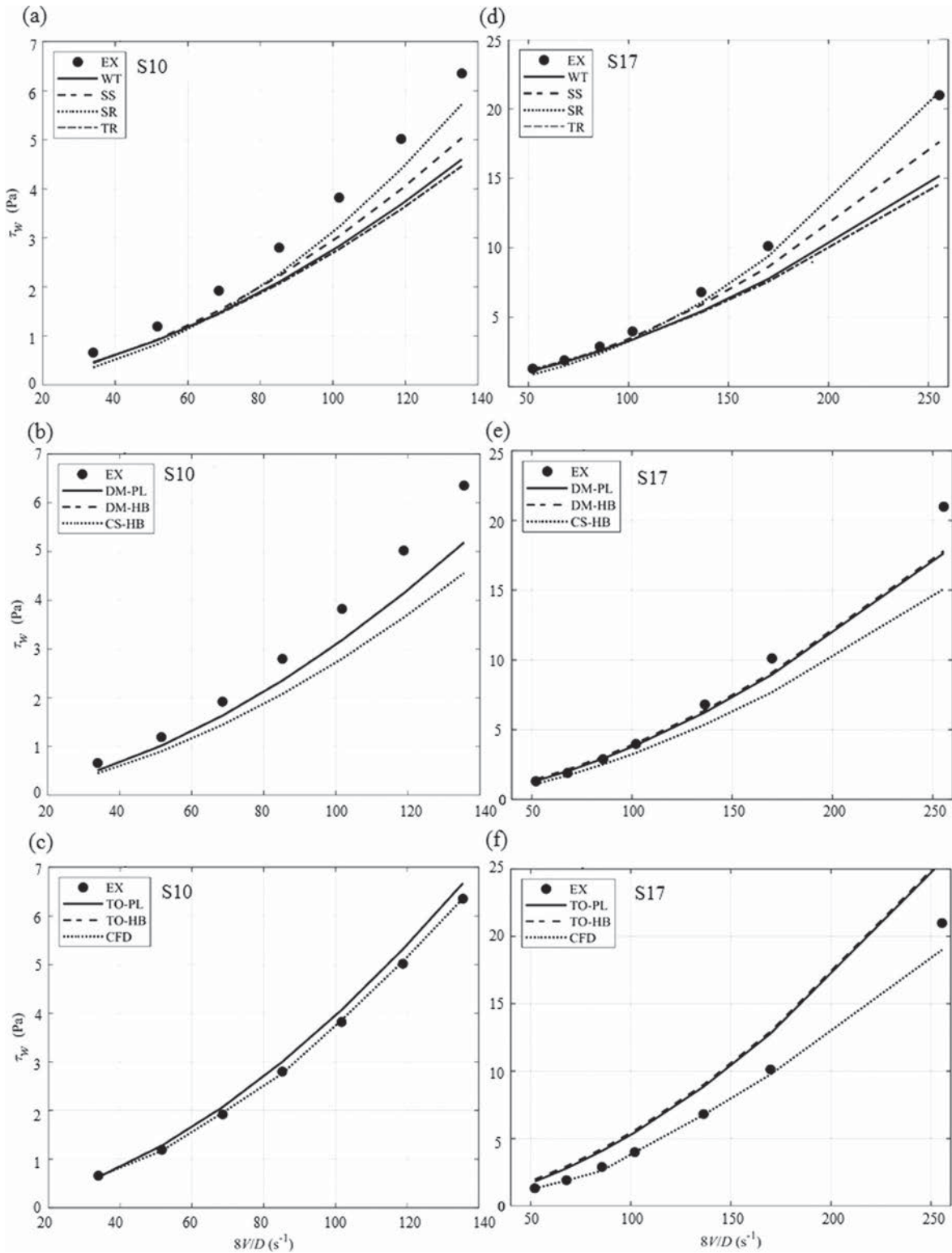
Figure 3　Shear stress vs. strain rate for S10 (left) and S17 (right). The graphs (a) & (d) correspond to the models WT, SS, SR & TR; (b) & (e) correspond to DM-PL, DM-HB & CS-HB and (c) & (f) correspond to TO-PL, TO-HB & CFD. In each graph, EX represents the experimental data points shown using solid black dots.

experimental value". The latter indicates the general accuracy of a numerical method, whereas the distribution itself will indicate the precision a numerical method delivers. This analysis could be taken further, by using the probability distributions of the experiments and the models, to estimate the probability of

how likely is a numerical method to provide accurate measurements upon repeated application (to a range of flow velocities, diameters and rheological properties), while accounting for the precision with which an experimental set-up can provide the real value.
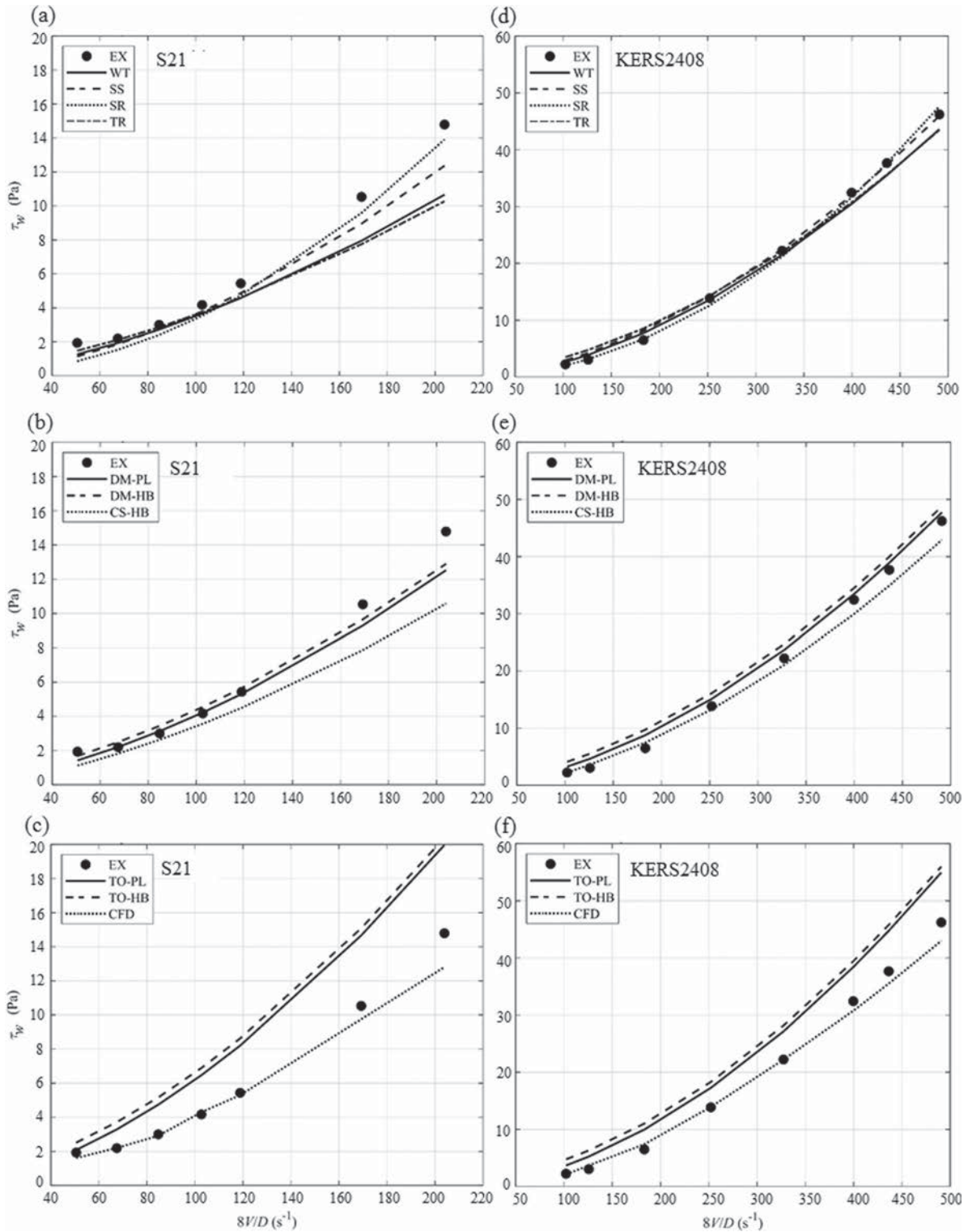
Figure 4   Shear stress vs. strain rate for S21 (left) and KERS2408 (right). The graphs (a) & (d) correspond to the models WT, SS, SR & TR; (b) & (e) correspond to DM-PL, DM-HB & CS-HB and (c) & (f) correspond to TO-PL, TO-HB & CFD. In each graph, EX represents the experimental data points shown using solid black dots.

This is further explained in terms of Fig. 5. The experimentally-determined wall shear stress is shown as EX with the dotted Gaussian curve representing the precision of the apparatus. Next for the entire set of experimental data points, i.e. every relation between wall shear and flow velocity across

the different HB fluids, one calculates the average of the difference between the experimental and numerical estimates and the standard deviation in this difference. Using these data, one obtains a Gaussian distribution for any model under consideration (shown as "Model" in Fig. 5 with the dashed line). This
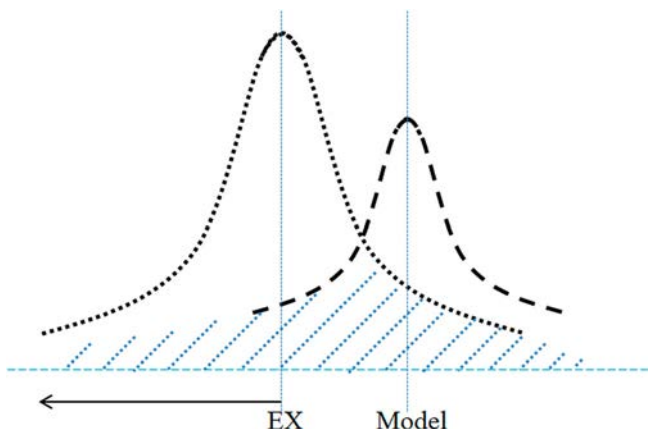
Figure 5   A schematic representation of the uncertainty analysis

Table 3   Probability of prediction

Model	Probability
CFD	0.27
Dodge and Metzner	0.22
Slatter	0.21
Torrance	0.14
Wilson and Thomas	0.13
Tomita	0.07

Table 4   Probability of prediction corrected with the operational envelope (Mehta et al., 2019)

Model	Probability
CFD	0.61
Dodge and Metzner	0.27
Slatter	0.26
Torrance	0.19
Wilson and Thomas	0.18
Tomita	0.11

is the precision that a numerical method can deliver (see Fornasini, 2008 for the mathematics underlying such analyses and possible applications).

Using the above, one can estimate the probability with which a numerical method can correctly estimate the wall shear stress within experimental bounds, by calculating the area common to the two Gaussian curves shown in Fig 5. The experimental bounds for the HB fluids S10 through S21 are mentioned in Section 4. Slatter (1995) also contains details on the errors incurred while studying the HB fluids KERS0608 and KERS2408. However, the error is not reported in terms of the standard deviations it represents.

Therefore, the error analysis detailed in this section is only carried out using the experimental data for S10 through S21, for which the experimental error corresponds to 2 standard deviations or 95% confidence. Using this approach, one obtains the probabilities listed in Table 3.

Although the probability is best with CFD, the overall values of all the numerical methods discussed in this article are, in fact, very low, with 0.27 being the maximum. It is interesting to note that the Dodge and Metzner approach based on dimensional analysis is nearly as accurate as CFD. Further, Slatter's approach, despite being tuned for a dataset which is not included in this error analysis, is as accurate as Dodge and Metzner's approach. All the other semi-empirical models demonstrate little accuracy in their estimates. The lowest accuracy is that of the Tomita model, which in fact is based on the treatment of turbulent non-Newtonian flows as though they were mathematically satisfying laminar flow conditions Skelland (1967).

Despite the above results, it is fair to mention that the CFD approach proposed in Mehta et al. (2018) works accurately only within a well-defined envelope that is described in Mehta et al. (2019). This operational envelope is bound by highly turbulent flows, and hence, high flow velocities (more than $1.5 \, \mathrm{m \, s^{-1}}$ or $8V/D$ more than $200 \, \mathrm{s^{-1}}$); and a value of yield stress that must be comparable with the wall shear stress. Accounting for these nuances and implementing the operational envelope to the probability analysis, one obtains the probabilities listed in Table 4.

All numerical approaches show improved accuracy upon restricting the range of velocities. However, CFD particularly shows a twofold improvement. With regard to the goals of our research, the best possible estimate of the pressure drop would provide a better insight in the energy demands in a sewer system designed to transport concentrated domestic slurry. Therefore, the low probabilities achieved by semi-empirical models require improvement. Even if one multiplies the estimates of the semi-empirical model by a factor of 1.5–2.0, which is common practice in engineering, the probabilities of estimating the wall shear stress and hence, the energy demands of a transport system, are far from being accurate and reliable for an efficient design. This makes estimating the wall shear stress of turbulent HB fluids a critical design parameter for systems carrying the same.

7   Discussion

It is important to discuss the results presented here by beginning with the statement that each of the numerical methods considered in this article only represents a part of or a simplified version of the physical phenomena concerning the turbulent flow of an HB fluid in a pipe.

Models based on simplification of the turbulent flow, such as Tomita's model that uses the laminar velocity profile to determine the extent of the plug region, tend not to be very accurate. Nonetheless, it is interesting to note that the extension of Tomita's PL model to HB fluids following the incorporation of the yield stress does not alter the estimates. This is solely because the shear stress near the wall has a greater contribution to the velocity profile, and near a wall the behaviour of both PL and HB fluids is dominated by their fluid behaviour indices,

as correctly hypothesized by Dodge and Metzner (1959). But one must bear in mind that this article considers a pipe with an inner diameter of 100 mm. In a practical situation, this diameter might change from 40–80 mm in households to 100–200 mm in the main transport lines, and the effects of these changes must also be accounted for.

On the other hand, the Wilson and Thomas model based on the fundamentals of turbulence and boundary layer thickness is only slightly more accurate (Tables 3 and 4) than Tomita's model for the cases considered in this article. Slatter's model, which was tuned for a set of experiments not included in error analysis, has an accuracy that is comparable with CFD.

CFD itself shows enhanced accuracy within the operational envelope determined using a strict sensitivity analysis (Mehta et al., 2019). However, it is fair to mention that the CFD approach mostly enforces a relation that the wall shear stress must bear with the velocity field near the wall, to satisfy the universal law of the wall modified to account for the viscosity of a non-Newtonian HB fluid. An experimental campaign that could support this relationship is still lacking, although the method itself has been validated for a wide range of test-cases concerning HB fluids, available in literature and for 3D flow situations that include a horizontal circular pipe followed by two right-angled bends (Mehta et al., 2018). Perhaps one reason why the CFD approach works well is that it complied with Dodge and Metzner's idea that a more fundamental treatment of the shear near the wall region is central to a better estimation of the flow that results. However, when used for a Newtonian fluid, CFD is capable of simulating the turbulent flow inside a pipe with very high accuracy for a range of RANS methods, as seen in existing literature.

8   Conclusions and outlook

Based on the tests outlined in this article, one can conclude that despite a number of approaches proposed so far, the numerical estimation of wall shear stress for turbulent HB fluids in circular pipes still remains a challenge, in contrast with the wide range of numerical methods readily available for the analysis of Newtonian flows.

Semi-empirical models are often based on the over-simplification of the physical aspects of non-Newtonian turbulent flows. Further, the use of a restricted set of experiments for the determination of any empirical parameters does hinder the ability of such models to be versatile. In this regard, extending Slatter's model to experiments beyond the ones considered in its formulation could perhaps make the model more robust and accurate, and hence, is worth investigating. Further, it is important to investigate a fundamental aspect of HB flows, i.e. the unyielding region at the centreline of a pipe, because some empirical models take the presence of this region into account and others do not. Additionally, experimental details on the velocity profile near the wall, based on a range of flow and rheological conditions, could also be useful for determining

a semi-empirical relationship between wall-stress, flow velocity and rheological parameters. Further, the current studies consider a pipe with an inner diameter of 100 mm. It would be interesting to know the effect of a larger pipe diameter on the flow profile.

Although our results indicate that CFD holds promise in terms of its capacity to estimate frictional losses, it requires further development in terms of incorporating the fundamentals of non-Newtonian turbulence, which themselves require thorough experimental investigation, given the lack of ample literature on the subject. The wall function that appears to be accurate within a restricted envelope also requires experimental verification and possible improvement. Finally, should CFD be improved to the extent that it becomes more accurate and reliable for estimating frictional losses in HB fluids, one will still require the computationally cheaper and simpler semi-empirical or reduced-order models to extend the calculations on a single circular pipe, to an entire urban sewer system, which is the motivation behind the research that concerns this article. The estimation of the frictional losses provides information on the energy required to transport a concentrated HB fluid, making it an important design parameter, and hence requiring more accurate and reliable mathematical models.

Appendix 1

This appendix provides details on the derivation of the wall function used to enable a CFD-based analysis of the pressure loss in a circular pipe carrying a turbulent HB fluid. As mentioned previously, for a Newtonian fluid:

$$\boldsymbol{\tau} = \mu \dot{\boldsymbol{\gamma}}^n \tag{A1}$$

Whereas, an HB fluid has a constitutive relationship of a the following form:

$$\boldsymbol{\tau} = \boldsymbol{\tau}_y + m \dot{\boldsymbol{\gamma}}^n \tag{A2}$$

The standard wall function proposed by Launder and Spalding (1974) took into account the shear stress in a Newtonian fluid to estimate the velocity in a grid point close to a wall boundary:

$$\frac{u}{\left(\frac{\boldsymbol{\tau}_w}{\rho}\right)^2} = \frac{1}{\kappa} \ln\left\{ \frac{y\rho E}{\mu} \left(\frac{\boldsymbol{\tau}_w}{\rho}\right)^{1/2} \right\} \tag{A3}$$

wherein κ is a constant that is nearly 0.4 and E is about 9.973. This was extended to account for the yield stress and the consistency and behavior indices of an HB fluids, using an analysis similar to the one followed by Launder and Spalding (1974) for a Newtonian fluids. One ends up with (Mehta et al., 2018):

$$\frac{u}{\left(\frac{\boldsymbol{\tau}_w - \boldsymbol{\tau}_y}{\rho}\right)^2} = \frac{1}{n\kappa}\ln\left\{\frac{y^n \rho E}{m}\left(\frac{\boldsymbol{\tau}_w - \boldsymbol{\tau}_y}{\rho}\right)^{(2-n)/2}\right\} \qquad (A4)$$

In the limit of vanishing yield stress and a behavior index $n = 1$, the above expression reduces to Launder and Spalding's equation for a Newtonian fluid. As mentioned in the main text, the above equation was validated using pressure drops across circular pipes (with bends too) obtained from experiments on a range of HB slurries. Further, an operating envelope wherein this equation provides reasonable estimates was proposed, thus, placing a limit on flow velocity, yield stress is to wall stress ratio and behavior index. Within these limits, the proposed wall function can safely be used in combination with $\kappa - \epsilon$ and Reynolds stress models.

Notation

A	=	model constant in Tomita's equation
A_n	=	constants as function of n in Dodge and Metzner's method (also B_n, C_n and P_n)
B	=	model constant in Tomita's equation
d_{85}	=	representative size of the particles in a slurry (μm)
D	=	pipe diameter (mm)
D_a	=	modified pipe diameter in Slatter's model (m)
f_*	=	modified friction factor
f_B	=	friction factor for a Bingham plastic fluid
f_H	=	friction factor for a Herschel–Bulkley fluid as per Tomita's method
f_{HB}	=	friction factor for a Herschel–Bulkley fluid as per Dodge and Metzner's method
f_N	=	Fanning friction factor for a Newtonian fluid
f_P	=	friction factor for a power law fluid
H	=	function of ζ for a Bingham plastic fluid
G	=	function of n for a power law fluid
H	=	function of ζ and n for a Herschel–Bulkley fluid
L	=	pipe length (m)
m	=	consistency index (Pa s^n)
m'	=	modified consistency index
n	=	behaviour index
n'	=	modified behaviour index
N_{Re}°	=	modified Reynolds number for a power law fluid
$N_{Re\text{-}Gen}$	=	generalized Reynolds number defined by Rabinowitsch and Mooney

$N_{Re\text{-}Gen_{HB}}$	=	generalized Reynolds number for Herschel–Bulkley fluids
$N_{Re\text{-}Gen_{PL}}$	=	generalized Reynolds number for power law fluids
p	=	static pressure (Pa)
Q	=	volumetric flow rate (l min^{-1})
r	=	arbitrary radial distance
r_p	=	radial extent of the plug from the centreline
R	=	arbitrary pipe radius
R_e	=	Reynolds number for a Newtonian fluid
Re_B	=	Reynolds number for a Bingham plastic fluid
Re_{Bi}	=	Bird's generalized Reynolds number for a power law fluid
Re_{CS}	=	Chilton and Stainsby's Reynolds number for a Herschel–Bulkley fluid
Re_H	=	Reynolds number for a Herschel–Bulkley fluid
Re_P	=	Reynolds number for a power law fluid
Re_R	=	Slatter's Reynolds number for a rough-walled pipe
Re_{Sl}	=	Slatter's Reynolds number for a smooth-walled pipe
u'	=	velocity fluctuation due to turbulence (also v')
$\boldsymbol{u}$	=	velocity vector
$v_{\boldsymbol{\tau}_H}$	=	friction velocity for a Herschel–Bulkley fluid
$v_{\boldsymbol{\tau}}$	=	friction velocity
v_*	=	modified velocity to account for the plug
v_p	=	plug velocity
V	=	average flow velocity (m s^{-1})
V_*	=	modified arbitrary average flow velocity
V_a	=	modified average flow velocity for Slatter's model (m s^{-1})
V_z	=	axial flow velocity at an arbitrary radial distance r
y	=	arbitrary perpendicular distance from a pipe's wall
Z	=	dimensionless constant in Dodge and Metzner's method
α_H	=	model constant in Tomita's Herschel–Bulkley model
$\dot{\boldsymbol{\gamma}}$	=	strain rate (s^{-1})
$\dot{\boldsymbol{\gamma}}_w$	=	strain rate at the wall
$\dot{\boldsymbol{\gamma}}$	=	strain rate tensor
Δ	=	difference
ϵ	=	rate of dissipation of turbulence kinetic energy per unit mass (m^2 s^{-3})
ζ	=	the ratio $\boldsymbol{\tau}_y/\boldsymbol{\tau}_w$
η	=	effective viscosity (Pa s)
η_w	=	wall effective viscosity (Pa s)
θ	=	a function of n and ζ for a Herschel–Bulkley fluid
κ	=	turbulence kinetic energy per unit mass (m^2 s^{-2})
μ	=	molecular viscosity (Pa s)
ξ	=	model constant in Dodge and Metzner's model
ρ	=	density (kg m^{-3})

σ	=	standard deviation
τ	=	shear stress (Pa)
τ_{rz}	=	shear stress along the pipe's axis on a face with the radius as the normal (Pa)
τ_w	=	wall shear stress (Pa)
τ_y	=	yield stress (Pa)
$\boldsymbol{\tau}$	=	shear stress tensor (Pa)
ϕ	=	a function of n and ζ for a Herschel–Bulkley fluid
ω	=	dissipation rate per unit turbulence kinetic energy (s^{-1})
ω	=	function of m' and n' in the Rabinowitsch and Mooney theory
BP	=	Bingham plastic
CFD	=	computational fluid dynamics
CS	=	Chilton and Stainsby
DM	=	Dodge and Metzner
HB	=	Herschel–Bulkley
PL	=	power law
RANS	=	Reynolds-averaged Navier–Stokes
RM	=	Rabinowitsch and Mooney
RSM	=	Reynolds stress model
SR	=	Slatter rough
SS	=	Slatter smooth
TO	=	Tomita
TR	=	Torrance
WT	=	Wilson and Thomas

Notes

1. Skelland (1967) is a general reference. For details on the similar relationships for the laminar flow of HB fluids, readers could refer to the review article by Heywood and Cheng (1984) and literature by Bird et al. (1987, 1983).
2. $\boldsymbol{\tau} = m\dot{\boldsymbol{\gamma}}^n$, $n \neq 1$ for power law fluids.
3. $\boldsymbol{\tau} = \boldsymbol{\tau}_y + m\dot{\boldsymbol{\gamma}}$ for Bingham plastics.

ORCID

Jules B. Van Lier http://orcid.org/0000-0003-2607-5425
Francois H.L.R. Clemens http://orcid.org/0000-0002-5731-0582

References

Assefa, K., & Kaushal, D. (2015). A comparative study of friction factor correlations for high concentrate slurry flow in smooth pipes. *Journal of Hydrology and Hydromechanics*, *63*(1), 13–20. https://doi.org/10.1515/johh-2015-0008

Bartosik, A. S. (2006). Modelling of a turbulent flow using the Herschel-Bulkley rheological model. *Chemical and Process Engineering - Inzynieria Chemiczna i Procesowa*, *27*, 623–632.

Bartosik, A. S. (2011). Simulation of the friction factor in a yield-stress slurry flow which exhibits turbulence damping near the pipe wall. *Journal of Theoretical and Applied Mechanics*, *49*, 283–300.

Bird, R. B., Armstrong, R. C., & Hassager, O. (1987). *Dynamics of polymeric liquids, vol. 1: Fluid mechanics* (2nd ed.). John Wiley & Sons.

Bird, R. B., Dai, G. C., & Yarusso, B. J. (1983). The rheology and flow of viscoplastic materials. *Reviews in Chemical Engineering*, *1*(1), 1–70. https://doi.org/10.1515/revce-1983-0102

Buckingham, E. (1914). On physically similar systems; illustrations of the use of dimensional equations. *Physical Review of the American Physical Society*, *4*, 345–376. https://doi.org/10.1103/PhysRev.4.345

Chabbra, R. P., & Richardson, J. F. (1999). *Non-newtonian flow in the process industries* (1st ed.). Butterworth-Heinemann.

Chilton, R. A., & Stainsby, R. (1998). Pressure loss equations for laminar and turbulent non-Newtonian pipe flow. *Journal of Hydraulic Engineering*, *124*(5), 522–529. https://doi.org/10.1061/(ASCE)0733-9429(1998)124:5(522)

Dodge, D. W., & Metzner, A. B. (1959). Turbulent flow of non-Newtonian systems. *AIChE Journal*, *5*(2), 189–204. https://doi.org/10.1002/(ISSN)1547-5905

Fornasini, P. (2008). *The uncertainty in physical measurements* (1st ed.). Springer-Verlag.

Herschel, W. H., & Bulkley, R. (1926). Konsistenzmessungen von Gummi-Benzollösungen. *Kolloid-Zeitschrift*, *39*(4), 291–300. https://doi.org/10.1007/BF01432034

Heywood, N. I., & Cheng, D. C. H.. (1984). Comparison of methods for predicting head loss in turbulent pipe flow of non-Newtonian fluids. *Transactions of the Institute of Measurement and Control*, *6*(1), 33–45. https://doi.org/10.1177/014233128400600105

Launder, B. E., & Spalding, D. B. (1974). The numerical computation of turbulent flows. *Computer Methods in Applied Mechanics and Engineering*, *3*(2), 269–289. https://doi.org/10.1016/0045-7825(74)90029-2

Malin, M. R. (1997). The turbulent flow of Bingham plastic fluids in smooth circular tubes. *International Communications in Heat and Mass Transfer*, *24*(6), 793–804. https://doi.org/10.1016/S0735-1933(97)00066-3

Malin, M. R. (1998). Turbulent pipe flow of Herschel-Bulkley fluids. *International Communications in Heat and Mass Transfer*, *25*(3), 321–330. https://doi.org/10.1016/S0735-1933(98)00019-0

Mehta, D., Thota-Radhakrishnan, A. K., van Lier, J., & Clemens, F. (2018). A wall boundary conditions for the simulation of a turbulent non-Newtonian domestic slurry in pipes. *Water*, *10*(2), 124. https://doi.org/10.3390/w10020124

Mehta, D., Thota-Radhakrishnan, A. K., van Lier, J., & Clemens, F. (2019). Sensitivity analysis of a wall boundary conditions for the turbulent pipe flow of Herschel-Bulkley

fluids. *Water*, *11*(1), 19. https://doi.org/10.3390/w110 10019

Metzner, A. B., & Reed, J. C. (1955). Flow of non-Newtonian fluidscorrelation of the laminar, transition and turbulent-flow regions. *AIChE Journal*, *1*(4), 434–440. https://doi.org/10.1002/(ISSN)1547-5905

Mooney, M. (1931). Explicit formulas for slip and fluidity. *Journal of Rheology*, *2*(2), 210–222. https://doi.org/10.1122/1. 2116364

Neill, R. I. G. (1988). *The rheology and flow behaviour of high concentration mineral slurries* [MSc Thesis]. University of Cape Town, Cape Town.

Nikuradse, J. (1933). Strömungsgesetze in rauhen RohrenStrömungsgesetze in rauhen Rohren. Forschung des Vereines Deutscher Ingenieure 361.

Oldroyd, J. G. (1947). A rational formulation of the equations of plastic flow for a Bingham solid. *Mathematical Proceedings of the Cambridge Philosophical Society*, *43*(1), 100–105. https://doi.org/10.1017/S0305004100023239

Prandtl, L. (1933). Neure Ergebnisse der Turbulenzforschung. *Zeitschrift des Vereines Deutscher Ingenieure*, *77*, 105–114.

Rabinowitsch, B. (1929). Über die Viskosität und Elastizität van SohlenÜber die Viskosität und Elastizität van Sohlen. *Zeitschrift für physikalische Chemie*, *145*, 1–26.

Skelland, A. H. P. (1967). *Non-Newtonian flow and heat transfer*. John Wiley & Sons.

Slatter, P. T. (1995). *Transitional and turbulent flow of non-Newtonian slurries in pipes* [Unpublished doctoral dissertation]. Department of Civil Engineering, University of Cape Town, Cape Town.

Thomas, A. D., & Wilson, K. C. (1987). New analysis of non-Newtonian turbulent flow - yield-power-law fluids. *The Canadian Journal of Chemical Engineering*, *65*(2), 335–338. https://doi.org/10.1002/cjce.v65:2

Thota-Radhakrishnan, A. K., van Lier, J., & Clemens, F. H. L. R. (2018). Rheological characterisation of concentrated domestic slurry. *Water Research*, *141*, 235–250. https://doi.org/10.1016/j.watres.2018.04.064

Tomita, Y. (1959). A study on non-Newtonian flow in pipe lines. *Bulletin of the Japan Society of Mechanical Engineers*, *2*(5), 10–16. https://doi.org/10.1299/jsme1958.2.10

Torrance, B. M. (1963). Friction factors for turbulent non-Newtonian fluid flow in circular pipes. *South African Mechanical Engineering*, *13*, 89–91.

Wilson, K. C., & Thomas, A. D. (1985). A new analysis of the turbulent flow of non-Newtonian fluids. *The Canadian Journal of Chemical Engineering*, *63*(4), 539–546. https://doi.org/10.1002/cjce.v63:4

Zeeman, G., & Kujawa-Roeleveld, K. (2011). Resource recovery from source separated domestic waste (water) streams; full scale results. *Water Science and Technology*, *64*(10), 1987–1992. https://doi.org/10.2166/wst.2011.562